Mantises exchange angular momentum between three rotating body parts to jump precisely to targets

by

Burrows, M. [1], Cullen, D.A. [1, 2,*], Dorosenko, M. [1] and Sutton, G.P. [3]

[1] Department of Zoology, University of Cambridge, Cambridge, CB2 3EJ, UK.
[2] Department of Biology, University of Leicester, Leicester, LE2 7RH, UK.
[3] School of Biological Sciences, University of Bristol, Bristol BS8 1UG, UK.
* Present address: Department of Biology, KU Leuven, Naamsestraat 59, 3000 Leuven, Belgium.

Summary

Flightless animals have evolved diverse mechanisms to control their movements in air, whether falling with gravity or propelling against it. Many insects jump as a primary mode of locomotion and must therefore precisely control the large torques generated during take-off. For example, to minimize spin (angular momentum of the body) at take-off, plant-sucking bugs apply large equal and opposite torques from two propulsive legs [1]. Interacting gear wheels have evolved in some and give precise synchronisation of these leg movements [2, 3]. Once airborne, either as a result of jumping or falling, further adjustments may be needed to control trajectory and orient the body for landing. Tails are used by geckos to control pitch [4, 5] and by *Anolis* lizards to alter direction [6, 7]. To orient when falling, cats rotate their body [8], while aphids [9] and ants [10, 11] manipulate wind resistance against their legs and thorax. Falling is always downwards, but targeted jumping must achieve many possible desired trajectories. Here we show that when making targeted jumps (which usually lasted less than a tenth of a second), juvenile, wingless mantises first rotated their abdomen about the thorax to adjust the centre of mass and thus regulate spin at take-off. Once airborne, they then smoothly and sequentially transferred angular momentum in four stages and in different directions between the flexible, jointed abdomen, the two raptorial front legs, and the two propulsive hind legs to produce a controlled jump with a precise landing. Experimentally impairing abdominal movements reduced the overall rotation so that the mantis either failed to grasp the target or crashed into it head first.

Results and Discussion

We analysed videos of 381 targeted jumps performed by 58 juveniles of all larval stages of the mantis, *Stagmomantis theophila*. The target was a vertical, 4 mm diameter black rod placed against a white background at distances of 1 to 2 body lengths from the edge of a platform on which the mantis stood (Fig. 1A, Movie 1 in Supplementary material). Juvenile stages superficially resemble adults, but because they do not have wings they rely on targeted jumping to navigate between the twigs and leaves of their heterogeneous arboreal environment. The morphometrics of 5th, 6th and 7th instar mantises and their jumping performance were analysed (Table 1). The form of the jump and the take-off velocities were similar for each instar despite the four-fold differences in mass. The following analysis focused on the 6th instar (three jumps by each of six individuals).

The first movements in preparation for a targeted jump were a sideways swaying of the head to scan the target and apparently determine its distance [12, 13]. The body then rocked

backwards and the abdomen curled upwards so that its tip pointed forwards (Fig. 1B). Propulsive forces were generated by depression of the proximal segments (trochantera and the closely linked femora) and extension of the more distal tibiae of the middle and hind legs. Thrust continued until both pairs of these legs were outstretched at take-off. During this acceleration phase, which lasted for 33.8 ± 1.1 ms (mean of means), the abdomen was curled forwards and upwards and the front legs were off the ground and were progressively rotated anti-clockwise about the trunk to project in front of the body (Fig. 1B; Supplementary material, video 1). During these propulsive movements the centre of mass (COM) of the whole mantis (calculated from the sum of the COMs of individual body parts; see Supplementary material) stayed on the longitudinal body axis (Fig. 1C). Take-off occurred at a velocity of 1.0 ± 0.1 m s^{-1} (mean of means). The force from the legs was applied below the COM, resulting in an anti-clockwise whole-body spin that set the appropriate body angle for a precise landing on the target.

To test that control of this directed take-off was attributable to rotational movements of the front legs and abdomen about the trunk, a model was constructed based on the detailed data of a single natural jump by a 6th instar mantis. The COM was followed under three conditions. First, natural jumps; second, simulated jumps with the abdomen fixed in its starting position; third, simulated jumps with the front legs fixed in their starting positions. In these two simulations other body parts were allowed to move in the same trajectory as recorded in the videos of natural jumping (Fig. 1C). In the model, if movement of the abdomen was excluded, the COM fell ventrally from the longitudinal axis of the thorax and moved closer to the line of action of the propulsive legs, thus reducing the total spin of the body and altering its angle relative to the target. By contrast, excluding movements of the front legs in the second simulation did not shift the COM from the body.

Once airborne towards a target that was 1.5 to 2 body lengths distant, the sequence of leg and abdominal movements was the same from mantis to mantis. The COM moved around but this had little effect on the trajectory because gravity always acts downwards through the COM, and thus generates no torque. The abdomen, front, and hind legs performed a series of clockwise and anti-clockwise rotations during which they exchanged angular momentum at different times and in different combinations. By contrast, the trunk underwent much smaller changes in its angular momentum, which were just sufficient to ensure that the mantis was oriented at the correct angle for landing on the vertical target. Air resistance [14] was calculated to exert a maximum spin of the body relative to the horizon of five degrees (~ 20% of the total) making the exchange of angular momentum the dominant factor governing the rotation of the mantis. The four distinct exchanges of angular momentum between these components are detailed in the following example jump.

First (I in Fig. 2A, B), during the initial 10 ms after take-off, the front legs continued their upwards and anti-clockwise (=positive) rotation and the hind legs their clockwise (=negative) rotation about the trunk (head and thorax). For example, at 5 ms the front legs had an angular momentum of 103 g mm^2 s^{-1} and the hind legs -32 g mm^2 s^{-1}. The abdomen changed direction from its initial slow clockwise rotation about the trunk to a similarly slow anti-clockwise rotation, giving it a negligible average angular momentum. The trunk had an angular momentum of 49 g mm^2 s^{-1}, giving a total angular momentum for the whole mantis of 139 g mm^2 s^{-1}. If the front legs had stopped rotating at this stage, then their angular momentum would have transferred to the trunk, resulting in a large increase in spin by the mantis from 0.6 to 2.3 degrees ms^{-1} relative to the horizontal.

Second (II), starting approximately 10 ms after take-off, the rotation of the front legs came to a halt, whilst the anti-clockwise rotation of the abdomen about the trunk increased. By 25 ms into the jump, 103 g mm^2 s^{-1} of angular momentum had been transferred from the front legs to the abdomen. The hind legs continued their clockwise rotation about the trunk with an angular momentum of -28 g mm^2 s^{-1} (Fig. 2A, B).

Third (III), a further 15 ms into the aerial trajectory and 40 ms after take-off, the rotation of the hind legs was reversed to the anti-clockwise direction, bringing them forwards into their landing position with 10 g mm^2 s^{-1} of momentum at 40 ms, rising to 97 g mm^2 s^{-1} at 60 ms. This was synchronised with a deceleration of the abdominal rotation towards an angular momentum of 36 g mm^2 s^{-1} at 60 ms and an opposing clockwise rotation of the front legs of approximately -29 g mm^2 s^{-1} (Fig. 2A, B). Again opposing rotations, this time of the front and hind legs, maintained a low angular momentum of the trunk about the horizontal.

Last (IV), during the final 10 ms before landing, the hind legs and abdomen stopped rotating. This was balanced by a sharp anti-clockwise rotation of the front legs with 78 g mm^2 s^{-1} of angular momentum (Fig. 2A, B). The net result of this entire sequence was that the trunk of the mantis spun by 50 degrees relative to the horizontal with a near-constant angular momentum, aligning itself perfectly for landing with the front and hind legs ready to grasp the target.

To assess possible variability in this sequence, 13 jumps by five 6th instar mantises to the vertical target 1.5 to 2 body lengths away were analysed in further detail. While airborne, the trunk rotated with an angular velocity of 0.9 ± 0.1 degrees ms^{-1} (mean of means ± s.e.m.), and the abdomen and the hind legs rotated more than twice as fast at 2.9 ± 0.3 and 2.3 ± 0.8 degrees ms^{-1} respectively. The largest variability in angular velocity was thus seen in the rotations of the hind legs, where the s.e.m. was approximately 25% of the mean compared to 10% for abdominal rotations. The time spent airborne for this group was 68.4 ± 3.4 ms.

Two experimental manipulations were made to analyse the mechanics of the jump. First, the target distance was reduced and the angular velocity of the trunk was measured. If the mantis is adjusting its rotations, then a shorter jump would have to be accompanied by a faster angular rotation of the trunk to align properly with the target. When jumping to a target one body length away, there were no anti-clockwise rotations of the abdomen and the hind legs that occurred in periods II and III in jumps to the more distant targets (Fig. 2). The mantis now rotated 64% faster at 1.4 ± 0.2 degrees ms^{-1} and spent 66% less time airborne (44.9± 3.8 ms) while still landing precisely on the target (mean of means for six 6th instar mantises each jumping three times, compared with 13 jumps by five mantises jumping to targets at 1.5 to 2 body lengths). The absence of leg and abdominal rotations here, accompanied by a higher rotation rate of the trunk, thus confirms a role for these rotations in reducing whole-body spin in the longer jumps, and also suggests that they are under active muscular control.

In the second manipulation, flexibility of the abdomen was reduced by super-gluing the segments together and this resulted in the mantises rotating at an angular velocity of 0.6 ± 0.2 degrees ms^{-1} (mean of means of 17 jumps by two 5th instar mantises). This rate of rotation was 57% slower than that of unimpeded mantises when jumping the same distance of one body length. A further consequence was that the experimentally modified mantises did not rotate enough to land with the appropriate orientation to the target and thus failed to grasp it. Some under-rotations even resulted in mantises hitting the target head-first before falling away from it (Fig. 1D, Supplementary material, video 2).

What mechanisms do other animals use when making a targeted jump? Primates swing their front limbs forward, the mass of which is sufficient to act as a counter-weight contributing to forward thrust [15, 16]. In the much lighter mantises, however, the swing of the front legs cannot contribute to thrust because of their small size [16, 17]. Other invertebrates stabilise their mid-air trajectories by altering aerodynamic drag, a very different mechanism that exploits air resistance to maintain a constant orientation. Locusts curl their abdomen to help stabilise take-off [18] and jumping spiders spin a drag line from their abdomen [19]. Some insects also use their hind legs as rudders when airborne [11, 20]. By contrast, while wind resistance increased the total angular momentum in the mantis, the rotation of the legs and abdomen kept the angular momentum of the trunk low (Figure 2B; compare teal and black lines). Conservation of angular momentum to achieve specific body orientations is exploited by lizards, the tails of which act as reservoirs of angular momentum [4-6], and by falling cats, which counter-rotate the front and hind parts of their bodies [8]. The mantis, however, uses four different exchanges of angular momentum between three different rotating and interacting body parts and, in doing so, reduces whole-body spin three-fold towards a constant value commensurate with reaching and landing precisely on a target.

Some other insects (albeit ones that fly) have structures that they use as gyroscopes to provide fast sensory feedback during rotational motions. These operate over a time scale of milliseconds in flies (the halteres [21]), or tens of milliseconds in moths (the antennae [22]). Mantises do not have halteres and their antennae are not large or mobile enough to match these feats. Moreover, while both halteres and antennae require Coriolis accelerations to measure angular velocity, mantises do not have structures that move in such a way as to generate and react to these forces (Supplementary Movie 1). An assessment that now needs to be made for the mantis is the role of neural control (feed forward or feedback) in these exchanges of angular momentum. When jumping variable distances, mantises were able to adjust their rotation rates to achieve precise landings. Can the mantis also alter the trajectory of its jump after take-off, in response to changes in its environment? These principles of angular momentum exchange and their underlying control mechanisms could be extrapolated to the design of jumping robots, which presents a significant engineering problem to which solutions are still in the early stages of successful implementation [23-25]. The mechanism described here, like gears [3], screws [26], and high-speed lever systems [27], represents another natural prototype of man-made devices.

Figure Subscripts
Figure 1
A. Photograph of a 6th instar mantis nymph. **B**. Selected images from a natural jump by a 6th instar nymph captured at 1000 frames s[-1]. The open triangles indicate a constant reference point in all frames. Take-off occurred at 0 ms and the target was reached 70 ms later. During the airborne trajectory the abdomen, front and hind legs rotated about the thorax. **C**. Stick diagrams of the changing positions of the trunk, abdomen, front legs (all black lines) and hind legs (orange lines) made by tracing individual frames at the times indicated during a natural jump. The arrows show the direction of rotation that would happen in a natural jump. The jump was then modelled with either the front legs (green), or the abdomen (pink) held constant in their starting positions, but with the hind legs (orange) moving as they did in a natural jump. The resulting effect on the calculated COM is indicated by the coloured circles; green and pink respectively for when the front legs or abdomen did not move. **D**. Single frame from a jump by

a 5th instar mantis in which the segments of the abdomen were glued together. The mantis did not rotate enough and hit the target with its head.

Figure 2
A. Changes in joint angles measured in each successive frame (1 ms intervals) from a video of a natural jump. **B**. Calculated changes in angular momentum of different body parts during the same jump. To produce continuous smooth curves of angular velocity, the angles of the thorax, raptorial front legs, abdomen, and hind legs were measured at each frame, fitted to 9th order polynomials which were then differentiated against time and used to generate curves of angular momentum (further details in Supplementary material). The vertical shaded regions show the four periods (I-IV, demarcated by fuzzy boundaries) of the jump which are described in the text. The front legs (green), hind legs (orange), trunk (black) and abdomen (pink) are indicated. The total momentum of the mantis is shown in teal. The inset cartoon shows the angles measured relative to the horizontal. Take-off occurred at 0 ms (yellow bar). The stick diagrams are tracings from frames of a video of the natural jump, to show the orientations of the different body parts at the times indicated by the vertical black lines. The coloured lines join the base of the body parts to their most distal points; the legs move in three dimensions and the abdomen curves. The paler colour shows the previous position of the body part and the coloured arrows the direction of movement.

Table 1

Jumping parameters for three jumps by each of six 5th, six 6th and six 7th instar mantises expressed as mean of means ± s.e.m.
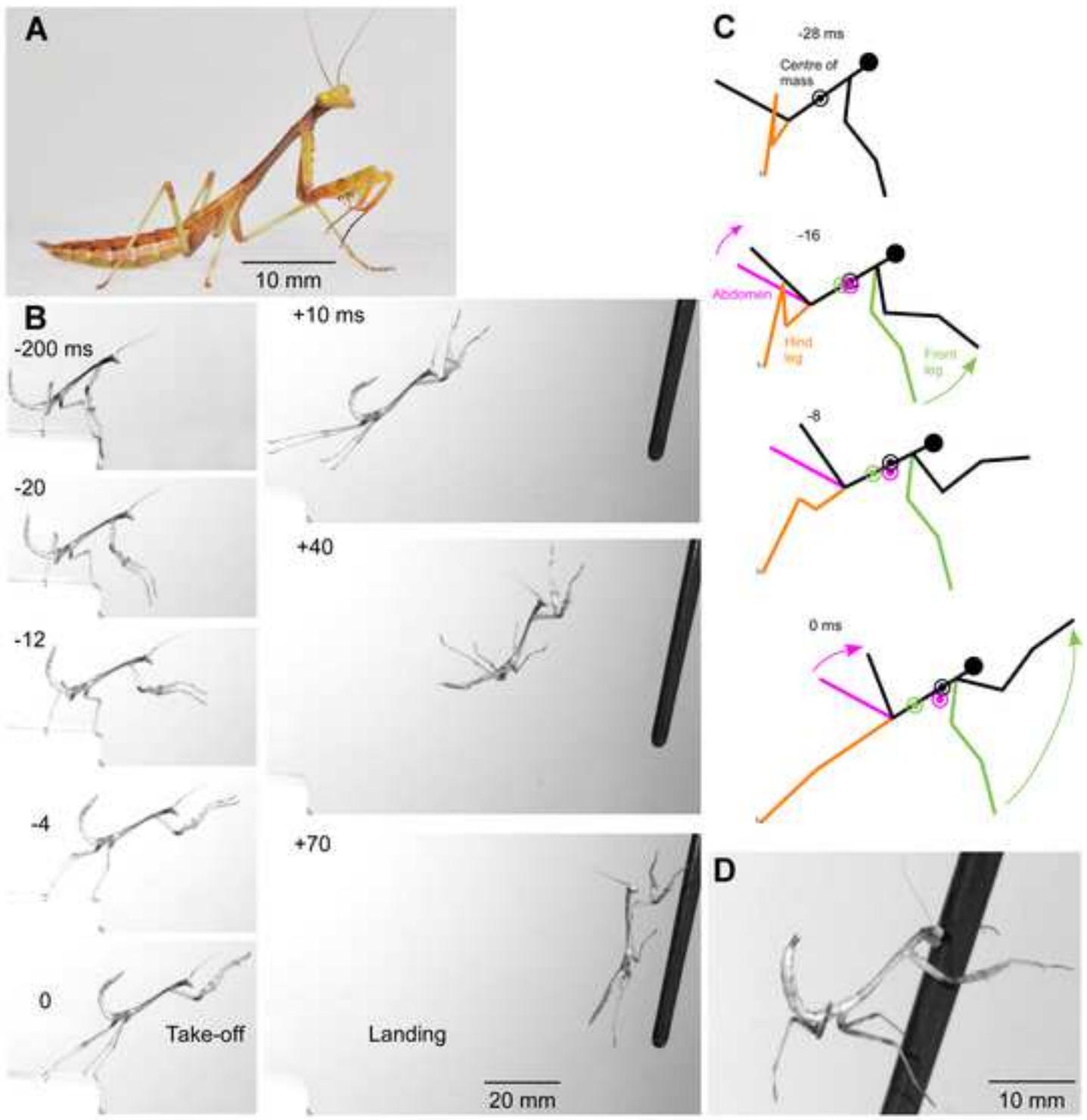
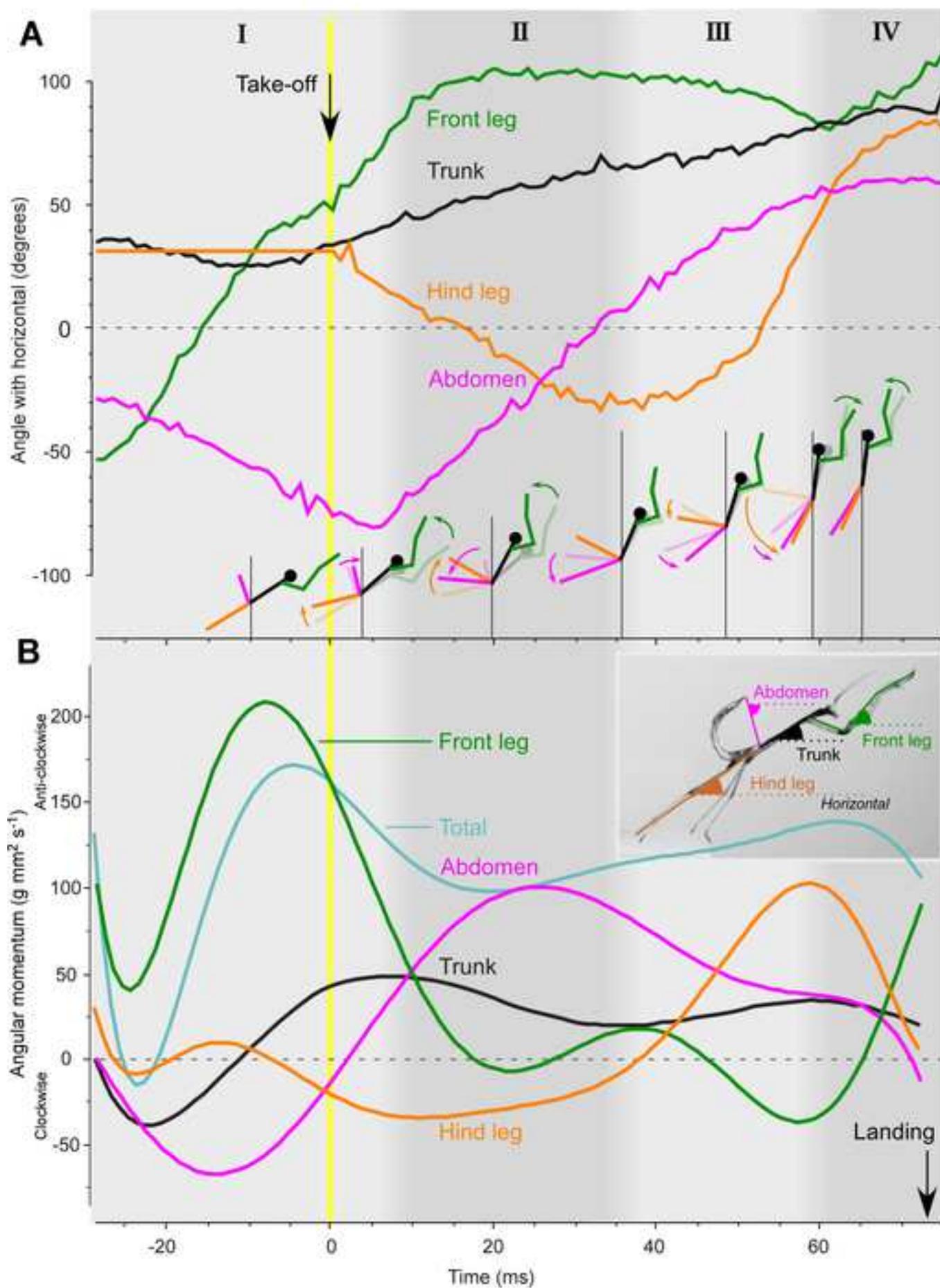|	Mass, mg	Body, length, mm	Front leg length, mm	Middle leg length, mm	Hind leg length, mm	Take off time, ms	Body angle at take-off, degrees	Take-off angle, degrees	Take-off velocity, m s^{-1}
5th instar	85.7 ± 6.9	30.5 ± 0.5	20.7 ± 0.6	15.7 ± 0.5	22.5 ± 0.5	30 ± 1.6	51.9 ± 2.1	45.6 ± 2.5	0.8 ± 0.1
6th Instar	172.1 ± 17.4	39.7 ± 1.6	27.8 ± 1.3	20.8 ± 0.7	28.6 ± 1.6	33.8 ± 1.1	41.1 ± 1.5	38 ± 2.4	1.0 ± 0.1
7th instar	355.6 ± 35.6	44.4 ± 0.5	30.2 ± 0.8	21.1 ± 2.4	29.9 ± 1.4	37.7 ± 1.7	45.3 ± 2.8	38.2 ± 3.3	1.0 ± 0.1

References

1. Sutton, G.P., and Burrows, M. (2010). The mechanics of azimuth control in jumping by froghopper insects. J. Exp. Biol. *213*, 1406-1416.
2. Burrows, M., and Bräunig, P. (2010). Actions of motor neurons and leg muscles in jumping by planthopper insects (Hemiptera, Issidae). J. Comp. Neurol. *518*, 1349-1369.
3. Burrows, M., and Sutton, G.P. (2013). Interacting gears synchronize propulsive leg movements in a jumping insect. Science *341*, 1254-1256.
4. Libby, T., Moore, T., Chang-Siu, E., Li, D., Cohen, D., Jusufi, A., and Full, R.J. (2012). Tail assisted pitch control in lizards, robots and dinosaurs. Nature *481*, 181-184.
5. Jusufi, A., Goldman, D.I., Revzen, S., and Full, R.J. (2008). Active tails enhance arboreal acrobatics in geckos. Proc. Natl. Acad. Sci. USA *105*, 4215-4219.
6. Gillis, G.B., Bonvini, L.A., and Irschick, D.J. (2009). Losing stability: tail loss and jumping in the arboreal lizard *Anolis carolinensis*. J. Exp. Biol. *212*, 604–609.
7. Higham, T.E., Davenport, M.S., and Jayne, B.C. (2001). Maneuvering in an arboreal habitat: the effects of turning angle on the locomotion of three sympatric ecomorphs of *Anolis* lizards. J. Exp. Biol. *204*, 4141-4155.
8. Diamond, J.M. (1988). Why cats have nine lives. Nature *332*, 586-587.
9. Ribak, G., Gish, M., Weihs, D., and Inbar, M. (2012). Adaptive aerial righting during the escape dropping of wingless pea aphids. Curr. Biol. *23*, R102.
10. Yanoviak, S.P., Dudley, R., and Kaspari, M. (2005). Directed aerial descent in canopy ants. Nature *433*, 624-626.
11. Yanoviak, S.P., Munk, Y., Kaspari, M., and Dudley, R. (2010). Aerial manoeuvrability in wingless gliding ants (*Cephalotes atratus*). Proc. R. Soc. B. *277*, 2199-2204.
12. Horridge, G.A. (1986). A theory of insect vision: velocity parallax. Proc. R. Soc. Lond. B *229*, 13–27.
13. Walcher, F., and Kral, K. (2008). Visual deprivation and distance estimation in the praying mantis larva. Physiol. Entomol. *19*, 230-240.
14. Bennet-Clark, H.C., and Alder, G.M. (1979). The effect of air resistance on the jumping performance of insects. J. Exp. Biol. *82*, 105-121.
15. Demes, B., and Gunther, M.M. (1989). Biomechanics and allometric scaling in primate locomtion and morphology. Folia Primatol. *53*, 125-141.
16. Zajac, F.E. (1993). Muscle coordination of movement: a perspective. J. Biomechanics *26*, 109-124.
17. Alexander, R.M. (1995). Leg design and jumping technique for humans, other vertebrates and insects. Philos. Trans. Roy. Soc. Lond. B *347*, 235-248.
18. Cofer, D., Cymbalyuk, G., Heitler, W.J., and Edwards, D.H. (2010). Control of tumbling during the locust jump. J. Exp. Biol. *213*, 3378-3387.
19. Chen, Y.-K., Liao, C.-P., Tsai, F.-Y., and Chi, K.-J. (2013). More than a safety line: jump-stabilizing silk of salticids. J. Roy. Soc. Interface *10*, 20130572.
20. Camhi, J.M. (1970). Yaw-correcting postural changes in locusts. J. Exp. Biol. *52*, 519-531.
21. Dickinson, M.H. (1999). Haltere-mediated equilibrium reflexes of the fruit fly, *Drosophila melanogaster*. Phil. Trans. Roy. Soc. Lond. B *354*, 903-916.
22. Sane, S.P., Dieudonne, A., Willis, M.A., and Daniel, T.L. (2007). Antennal mechanosensors mediate flight control in moths. Science *315*, 863-866.
23. Noh, M., Kim, S.-W., An, S., Koh, J.-S., and Cho, K.-J. (2012). Flea-inspired catapult mechanism for miniature jumping robots. IEEE Trans. Robot. *28*, 1007-1018.
24. Zhang, J., Song, G., Li, Y., Qiao, G., Song, A., and Wang, A. (2013). A bio-inspired jumping robot: Modeling, simulation, design, and experimental results. Mechatronics *23*, 1123–1140.
25. Churaman, W.A., Gerratt, A.P., and Bergbreiter, S. (2011). First leaps toward jumping microrobots. In 2011 IEEE/RSJ International Conference on Intelligent Robots and Systems September 25-30, 2011. (San Francisco, CA, USA).

26.   van de Kamp, T., Vagovič, P., Baumbach, T., and Riedel, A. (2011). A biological screw in a beetle's leg. Science *333*, 52.

27.   Robert, D., Miles, R.N., and Hoy, R.R. (1998). Tympanal mechanics in the parasitoid fly *Ormia ochracea*: intertympanal coupling during mechanical vibration. J. Comp. Physiol. [A] *183*, 443-452.

Figure 1
Click here to download high resolution image

Figure 1

A

10 mm

B

-200 ms

-20

-12

-4

0

Take-off

+10 ms

+40

+70

Landing

20 mm

C

-28 ms

Centre of mass

-16

Abdomen

Hind leg

Front leg

-8

0 ms

D

10 mm

Figure 2

Supplementary Material

Supplementary Movie 1

A jump by a male 6th instar mantis captured at 1000 images s^{-1} with an exposure time of 0.2 ms and replayed at a rate of 30 images s^{-1}.

Supplementary Movie 2

A jump by a female 5th instar mantis captured at 1000 images s^{-1} with an exposure time of 0.2 ms and replayed at a rate of 30 images s^{-1}. The abdominal segments were glued together, resulting in the mantis hitting the target with its head but failing to grasp it.

Supplementary Figure 1

A. Diagram of the body parts used to calculate the centre of mass (COM) of the body in jumping. B. Diagram of the four body parts used to calculate angular momentum. See also Supplementary Table 1. R_{th} and R_h are the distances of the COM of the thorax and the head from the combined COM of the whole mantis. The colour coding is the same as used in text Figures 1 and 2.

Supplementary Table 1

Table of body parts, values, and formulae used to calculate the COM and the angular momenta of a jump by a 6th instar mantis. In columns 1 and 2, a-f refer to the body parts illustrated in Supplementary Figure 1.

Material and Methods

Animals

Stagmomantis theophila Rehn, 1904 (order Mantodea, family Mantidae) were bred from 5 adult males and 4 adult females. They were raised in individual containers and fed adult *Drosophila melanogaster* or early nymphs of the locust *Schistocerca gregaria*. Fifty eight individuals were followed from 1st instar juveniles to adulthood and their performance was analysed in 381 jumps. Males went through 7 juvenile instars before reaching adulthood whereas females had an additional eighth instar. Functional wings appeared only at the final moult to adulthood in both females and males.

Kinematics

Sequential images of jumps were captured at rates of 1000 s^{-1} and an exposure time of 0.2 ms with a single Photron Fastcam SA3 camera (Photron (Europe) Ltd, West Wycombe, Bucks., UK) fitted with a 100 mm macro Tokina lens. The images had a resolution of 1024 x 1024 pixels and were fed directly to a computer for later analysis. Jumps were made from a platform made of high density white foam (Plastazote, Watkins and Doncaster, Cranbrook, Kent, UK) 85 mm deep and 150 mm long against a white surrounding background. The target was a 4 mm diameter, 150 mm long, black rod held vertically against a white featureless background. The distance to the target was critical and depended on the age of the mantis; if the rod was too close it would be grabbed by the front legs and if too far from the edge of the platform the mantis would not jump to it. For the 6th instar mantises the target was 60-80 mm (1.5 to 2 body lengths) or 40 mm (1 body length) from the edge

of the platform. The target was positioned to ensure that jumps were parallel to the image plane of the camera. Selected image files were analysed with Motionscope camera software (Redlake Imaging, Tucson, AZ, USA) or with Canvas 14 (ACD Systems International Inc., Seattle, WA, USA). Take-off was designated as t = 0 ms and was defined as the time at which the last leg lost contact with the platform and the mantis became airborne. The acceleration time of a jump was defined as the period from the first detectable, propulsive movement of the middle and hind legs until take-off. Peak velocity was calculated as the distance moved in a rolling 3-point average of measurements taken from successive images, and the values presented are those reached just before take-off. Clockwise and anti-clockwise rotations of the body parts are used to describe jumps from left to right as viewed from the side. Measurements are given as means $\pm$ standard error of the mean (s.e.m). Temperatures for all experiments ranged from 25-30° C.

Modelling
Calculation of the centre of mass
To calculate the position of the centre of mass (COM), the body of the mantis was treated as 6 individual body parts (Supplementary Figure 1 and Supplementary Table 1): a) Trunk (head, thorax, middle legs). b) Abdomen. c) Front leg coxae. d) Front leg femora. e) Front leg tibiae/tarsi. f) Hind legs. The geometry of each part was modelled as indicated in column 3 of Supplementary Table 1.

At each frame (1 ms intervals), measurements of angles (Supplementary Figure 1) were mapped onto the simulated parts. The COM of each part was calculated and then multiplied by its mass. The algebraic mean of all these products was then calculated to find the COM of the whole mantis. Algebraically, the COM (X_{COM}, Y_{COM}) is expressed thus:

$$(1) \quad X_{COM} = \frac{\sum M_i X_i}{\sum M_i} \qquad Y_{COM} = \frac{\sum M_i Y_i}{\sum Y_i}$$

Where:
i is an index designating body parts a - f
M is mass
X is the x coordinate
Y is the y coordinate

Calculations were performed in Mathematica 5.0.

Calculation of Angular Momentum
Angular momentum (Supplementary Table 1) was calculated from the formula
$$(1) \quad \text{Angular Momentum} = \omega I$$
Where:
ω is the rate of change of angle of the body part (radians s^{-1})
I is the moment of inertia of the body part about its centre of rotation.

To calculate the moments of inertia (I) the body of the mantis was modelled as four parts (Supplementary Table 1); 1) Trunk (head, middle legs and thorax). 2) Abdomen. 3) Raptorial front

legs. 4) Hind legs. Since the pair of front legs both moved together, as did the pair of hind legs, each pair was modelled as a single entity.

To calculate angular velocity, the angles of the thorax, raptorial front legs, abdomen, and hind legs were measured at each frame (Text Figure 1) and fitted to 9th order polynomials which were then differentiated against time to produce continuous smoothed curves from which the angular velocity of each part was determined for each frame of the jump. This method of approximating angular velocity creates discontinuities at the edges of the simulation (-29 ms, 0 ms and +80 ms) and makes estimates of angular momentum unreliable at these times.

To calculate angular momentum, the moment of inertia of a body part was multiplied by its angular velocity. The units for these calculations were angular velocity in radians s^{-1}, mass in mg, moment of inertia in mg mm^2, and angular momentum in mg mm^2 s^{-1}. For ease of interpretation, angles are expressed in degrees and angular velocity in degrees ms^{-1}. To maintain unit consistency, the data for angular momentum should be presented in mg mm^2 s^{-1} but this would present large numbers. The units were therefore changed to g m^2 s^{-1} to remove a factor of 10^3. The simulation was run in Mathematica 5.0.

To estimate drag on the mantis during a leg motion, the drag force (F_d) was taken from the equation:

$$(1) \qquad F_d = \frac{1}{2} \, \rho \, V^2 \, C_d \, A$$

Where:
ρ is the density of air (1.26 kg m^{-3})
V is the velocity of a leg through the air (1 m s^{-1})
C_d is the drag coefficient of a cylinder (.82)
A is the planar area of a leg (104 * 10^{-6} m^2).

This estimate returns a force of 5.2 * 10^{-6} N on a leg.

This force was then approximated as acting through the COM of a leg, giving the force a moment arm of 13 * 10^{-3} m, and an approximate torque due to drag on a leg of 6.8 * 10^{-8} N.

This torque was then assumed to be transferred completely to the trunk – resulting in an angular acceleration (α) of:

$$\alpha = \text{Torque/Inertia}$$

Where:
the inertia of the trunk is 2.42 * 10^{-9} kg m^2 (Supplementary Table 1).

The net angular acceleration from this calculation is 28.0 radians s^{-2}, or 1517 degrees s^{-2}. Using a linear approximation of acceleration (angle = $\frac{1}{2}$ acceleration * $time^2$), the net change in angle caused by drag on the hind legs was 4.9 degrees over the period that the mantis was airborne. The hind legs

have the largest moment arm relative to the centre of mass, and consequently wind drag on them would result in the largest torque on the mantis. Several assumptions were added to ensure that this calculation would continue to over-estimate the amount of rotation due to wind drag on the hind legs:

1) The legs are assumed to be perpendicular to the flow throughout the entire jump.
2) The legs are assumed to be at their maximum distance from the centre of mass throughout the entire jump.
3) The torque is assumed to be transferred completely to the trunk and not distributed across the legs, abdomen, and trunk.
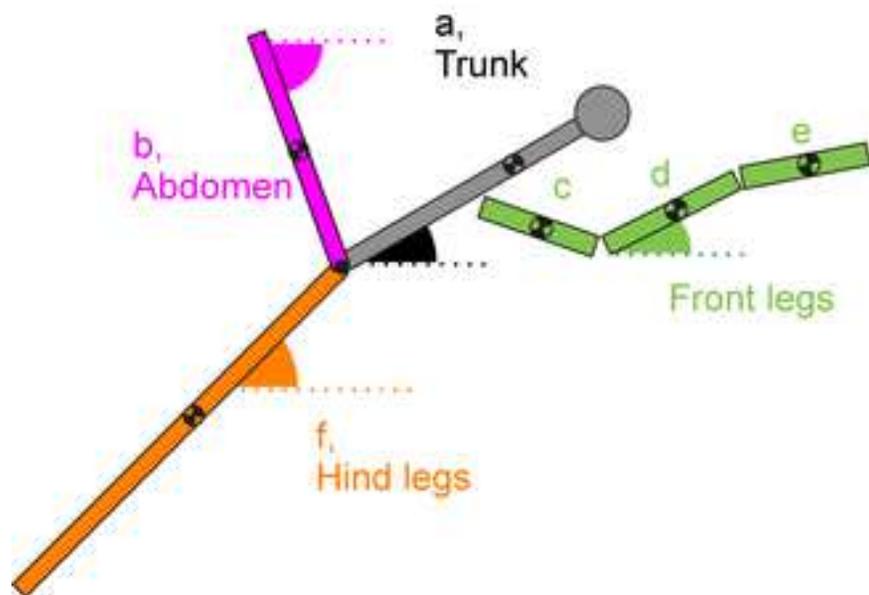
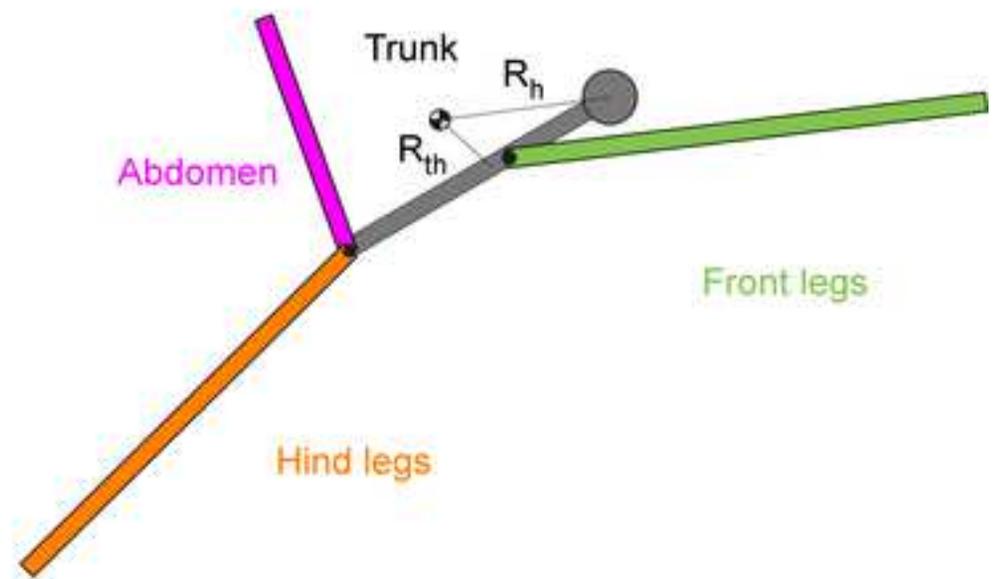| Body part	Body part subdivision	Geometry	Mass (M, mg)	Length (L, mm)	Inertia Formula*	Inertia, (mg.mm^2)	Angular velocity at highest momentum (deg ms^{-1})	Time at maximum momentum (ms)	Maximum angular momentum
Trunk, **a**	Thorax	Cylinder rotating about COM	53	17	$1/12\ ML^2$ $+ MR_{th}^2$	1570	0.9	-	27
	Middle legs		6						
	Head	Point mass rotating about COM	12	-	MR_h^2	850	0.9	-	15
	Total		**71**	**17**		**2420**	**0.9**	**17**	**42**
Abdomen, **b**	-	Cylinder rotating about its end	**28**	**14**	$1/3\ ML^2$	**1830**	**3.2**	**26**	**110**
Raptorial front legs	Coxae, **c**	Tapered cylinder rotating about its end	6	8	$1/4\ ML^2$	-	-	-	-
	Femora, **d**		7	9		-	-	-	-
	Tibiae/tarsi, **e**		6	8		-	-	-	-
	Total		**19**	**25**		**2970**	**2.5**	**75**	**130**
Hind legs, **f**	-	Tapered cylinder rotating about its end	**6**	**26**	$1/4\ ML^2$	**1010**	**5.4**	**58**	**100**

*During the aerial phase, the COM moved and as a consequence the moment of inertia changed by $\pm$ 6%

Supplementary Material Figure 1

A — Centre of mass

a, Trunk
b, Abdomen
c
d
e
Front legs
f, Hind legs

B — Angular momentum

Trunk
R_h
R_{th}
Abdomen
Front legs
Hind legs

Movie 1

Click here to download Supplemental Movie and Spreadsheet: Movie 1.mov

Movie 2

Click here to download Supplemental Movie and Spreadsheet: Movie 2.mov